Geomechanics and Engineering, *Vol. 17, No. 1 (2019) 57-67*
DOI: https://doi.org/10.12989/gae.2019.17.1.057

Effects of water on rock fracture properties: Studies of mode I fracture toughness, crack propagation velocity, and consumed energy in calcite-cemented sandstone

Varun Maruvanchery[1a] and Eunhye Kim[*1,2]

[1]*Underground Construction and Tunneling Engineering, Colorado School of Mines, Golden, Colorado, U.S.A.*
[2]*Department of Mining Engineering, Colorado School of Mines, Golden, Colorado, U.S.A.*

(Received April 13, 2018, Revised November 30, 2018, Accepted December 10, 2018)

Abstract. Water-induced strength reduction is one of the most critical causes for rock deformation and failure. Understanding the effects of water on the strength, toughness and deformability of rocks are of a great importance in rock fracture mechanics and design of structures in rock. However, only a few studies have been conducted to understand the effects of water on fracture properties such as fracture toughness, crack propagation velocity, consumed energy, and microstructural damage. Thus, in this study, we focused on the understanding of how microscale damages induced by water saturation affect mesoscale mechanical and fracture properties compared with oven dried specimens along three notch orientations-divider, arrester, and short transverse. The mechanical properties of calcite-cemented sandstone were examined using standard uniaxial compressive strength (UCS) and Brazilian tensile strength (BTS) tests. In addition, fracture properties such as fracture toughness, consumed energy and crack propagation velocity were examined with cracked chevron notched Brazilian disk (CCNBD) tests. Digital Image Correlation (DIC), a non-contact optical measurement technique, was used for both strain and crack propagation velocity measurements along the bedding plane orientations. Finally, environmental scanning electron microscope (ESEM) was employed to investigate the microstructural damages produced in calcite-cemented sandstone specimens before and after CCNBD tests. As results, both mechanical and fracture properties reduced significantly when specimens were saturated. The effects of water on fracture properties (fracture toughness and consumed energy) were predominant in divider specimens when compared with arrester and short transverse specimens. Whereas crack propagation velocity was faster in short transverse and slower in arrester, and intermediate in divider specimens. Based on ESEM data, water in the calcite-cemented sandstone induced microstructural damages (microcracks and voids) and increased the strength disparity between cement/matrix and rock forming mineral grains, which in turn reduced the crack propagation resistance of the rock, leading to lower both consumed energy and fracture toughness (K_{IC}).

Keywords: mode I fracture toughness; crack propagation velocity; consumed energy; water saturation; digital image correlation (DIC); microstructural damage

1. Introduction

Crustal rocks are constantly exposed to significant amount of water and various interstitial fluids (Fyfe *et al.* 1978). In general, natural rocks contain water molecules ranging from a few ppm (part per million) to several hundred ppm, and some traces of water molecules exist as structural defects (Behrens and Müller 1995). Structurally bound water (or hydrogen) can significantly influence the mechanical properties of minerals. Water is known to have a negative effect on mechanical properties, short- and long-term behavior of rocks (Hadizadeh and Law 1991, Schumacher and Kim 2013, Verstrynge *et al.* 2014). The presence of water especially in clay-rich rocks weakens the cementing or matrix material, increases pore water pressure, and enhances water-clay interaction, leading to a reduction in strength by creating microstructural damage in rocks (Erguler and Ulusay 2009, Karakul and Ulusay 2013).

For many decades, extensive research has been conducted to understand the effects of water on the strength and modulus of different rock types since understanding the effects of water on rock mechanics is critical to improve the design of geostructures. Some water-weakening mechanisms have been proposed to explain the influence of water on rock strength and modulus (Shakoor and Barefield 2009, Le *et al.* 2014, Kim and Changani 2016). The water-weakening mechanisms can be mainly grouped into physical effects and chemical effects. The physical effects include capillary tension, surface energy reduction and increase in pore pressure (Hawkins and McConnell 1992; Vásárhelyi and Ván 2006). The chemical effects of water are mostly by hydrolysis, dissolution, and oxidation (Weaver 1989, Feng *et al.* 2004). Apart from strength and modulus, fracture toughness is also one of the most important intrinsic material properties and can vary with the water content of rocks (Liu and Chen 2015). To assess rock fracture behaviors, fracture toughness has been widely used as a key indicator to estimate the resistance of rock to

∗Corresponding author, Assistant Professor
E-mail: ekim1@mines.edu
[a]Ph.D. Student

http://www.techno-press.org/?journal=gae&subpage=7 ISSN: 2005-307X (Print), 2092-6219 (Online)

fracture, and several testing methods have been employed to determine the fracture toughness of rocks (Nasseri and Mohanty 2008). The theory of fracture toughness has been developed mostly on the assumption of linear elasticity (Detournay 2016). Linear elastic fracture mechanics can be expressed as the critical stress intensity factor (K_{IC}), energy release rate (G_c), stress level (σ), and crack size (a) using following equations

$$\sigma = \sqrt{EG_c/\pi a} \quad \text{and} \quad \sigma = K_{Ic}/(a\sqrt{\pi a}) \tag{1}$$

K_{IC} represents critical stress intensity factor for plane strain condition, which is independent of sample thickness (still dependent on width and crack length) as a material constant, fracture toughness (Anderson 2017). K_{IC} is referred to as 'plane strain fracture toughness' and independent to the size of a sample. There are nearly always some levels of triaxiality along crack fronts except a very thin foil material where plane stress fracture typically occurs. Typical stress intensity factor (K)-controlled fracture occurs when a plastic zone is embedded within an elastic singularity zone for K. Although K is not valid as a characterizing parameter under fully plastic conditions, fracture toughness can be estimated with J integral or crack tip opening displacement (Labuz *et al.* 1985). In addition, T-stress and cohesive zone model have been used with consideration of the plastic behavior of fracture mechanics (Nara *et al.* 2011, Yoneyama *et al.* 2014, Gupta *et al.* 2015, Knauss 2015, Tracy *et al.* 2015, Gonzáles *et al.* 2017). However, despite many studies of rock fracture behaviors with the changes of water contents (Lim *et al.* 1994, Feng *et al.* 2009, Zhang 2016), the effects of water on the fracture toughness, crack propagation velocity, and consumed energy have not been sufficiently studied depending on bedding plane anisotropy.

Thus, in this study calcite-cemented sandstone specimens were tested to understand effects of water on rock fracturing behaviors as calcite mineral is extremely sensitive to water. The presence of water in calcite minerals converts strong silica-oxygen bonds into much weaker hydrogen bonds, and this phenomenon occurs at crack tips under a load (Dyke and Dobereiner 1991). The objectives of this study are to: (1) examine the reduction in mode I fracture toughness (K_{IC}), consumed energy and crack propagation velocity in calcite-cemented sandstone due to water saturation, (2) discover the relationship between K_{IC} and consumed energy, and (3) analyze microstructural damages produced in water-saturated specimens before and after loading tests. Consequently, our results in this paper provide insightful information for the advanced design and safety of geo- and infrastructures.

2. Materials and methods

2.1 Preparation of rock specimens

Several calcite-cemented sandstone blocks used in this study were quarried from Monroe County, Indiana. The rocks at this site belong to the sedimentary formations of Buffalo Wallow group of upper Mississippian age about 320-325 Ma. The rock formation in Buffalo Wallow group comprises of alternating layers of sandstone, shale and limestone (Thompson *et al.* 2013). Rock specimens for this study were prepared from the calcite-cemented sandstone block (1 m × 1 m × 1.2 m) by drilling both parallel and perpendicular directions to the bedding plane. The diameter of drilled cores was 57.1 mm. Specimens were prepared to measure their porosity, density, uniaxial compressive strength (UCS), indirect tensile strength (BTS), and mode I fracture toughness by using cracked chevron notched Brazilian disk (CCNBD). Specimens were divided into two groups; first group was incubated in a dry oven (105℃) for 24 h. The heating rate in the oven was maintained at 2.3℃ min^{-1} until reaching 105℃, and the specimens were kept at a constant temperature of 105℃ for 24 h. The specimens were slowly cooled in the oven to room temperature (RT) and tested. The second group was soaked in water for 48 h inside a vacuum chamber (70 kPa vacuum pressure) before loading tests. After 48 h, the saturated specimens were taken out from the vacuum chamber, surface-dried using a paper towel and tested.

2.2 Measurements of porosity and grain size

Porosity and density of the calcite-cemented sandstone specimens were assessed using saturation and caliper techniques as suggested by ISRM and others (Kim *et al.* 2017). Porosity of a rock is the ratio of pore volume to the total volume, so the porosity can be calculated as follows

$$\text{Porosity}, n = \frac{V_v}{V} * 100\% = \frac{\left(\frac{M_{sat} - M_{dry}}{\rho_w}\right)}{V} * 100\% \tag{2}$$

where V_v is the pore volume, V is the total volume, M_{sat} is the mass of a saturated sample, M_{dry} is the mass of a dry sample, and ρ_w is the density of water.

Density of a rock is the ratio of mass to the total volume and can be calculated as follows

$$\text{Density}, \rho = \frac{M}{V} \tag{3}$$

where M is the mass of a sample, and V is the total volume.

2.3 Uniaxial compressive strength (UCS), Brazilian tensile strength (BTS) and cracked chevron notched Brazilian disk (CCNBD)

UCS, BTS and CCNBD tests were performed with a servo-controlled hydraulic rock compression system (MTS). The specimens for different tests were initially cut to the required length using a saw. The length-to-diameter (L/D) ratios of specimens for UCS, BTS and CCNBD tests were 2.3, 0.5 and 0.47 respectively in accordance with ASTM and ISRM standards (Fowell and Xu 1994, ASTM D4543-08 2008, ASTM D3967-16 2016). For CCNBD specimens, chevron notch was made with two cuts from both sides of the specimen using a diamond-cutting blade. After making the first cut, specimen was rotated 180° along the diametrical axis to make the second cut. The cutting depth was determined according to the specimen diameter and the dimensionless geometric parameters such as α0, α1 or αB as suggested by Fowell and Xu (1994). Displacement control

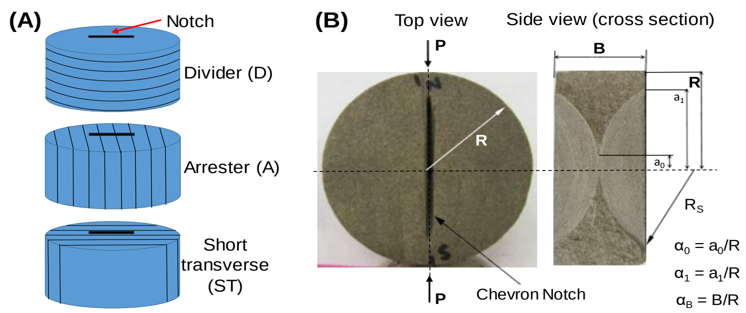

Fig. 1 Sample geometry and bedding plane orientations of CCNBD samples. (A) Three bedding plane orientations of CCNBD samples (divider, arrester, and short transverse) and (B) geometry of CCNBD specimen recommended by ISRM modified after Fowell (1995)

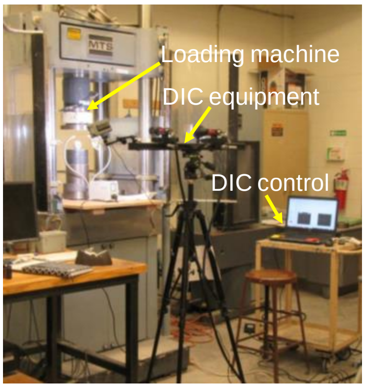

Fig. 2 Photo image of DIC setup for CCNBD specimen tests

mode was used for all the tests, and each specimen was loaded to failure at a displacement rate of 0.01 mm s^{-1}. UCS and BTS tests were conducted by dividing the specimens in two groups – according to the environmental condition (oven-dried and water-saturated) and the orientation of bedding plane (parallel and perpendicular). The peak load (P_{max}) after each test was noted, for calculating the UCS and BTS values of calcite-cemented sandstone. Tangent Young's modulus (E_{t50}) was also computed using the stress-strain curves obtained from the UCS tests.

CCNBD tests were conducted in accordance with the ISRM suggested standard (Fowell 1995, Chang *et al.* 2002) to examine mode I fracture toughness (K_{IC}). The specimens were divided into two groups; one ground was oven-dried specimens and the other group was water-saturated as described above. According to the orientation of a chevron notch with respect to the bedding planes, each group of the specimens was further divided into three groups-divider, arrester and short transverse (Fig. 1(A)) (Schmidt 1976). Specimens for fracture toughness tests were prepared carefully as proposed by ISRM. In this study, for calcite-cemented sandstone discs, average thickness (B) was 26.5 mm, initial chevron crack notch half-length (a_0) was 5.5 mm, final chevron notched crack half-length (a_1) was 22.3 mm, and radius (R) was 28.5 mm as illustrated in Fig. 1(B).

2.4 Digital image correlation (DIC) technique

Digital Image Correlation (DIC) is a non-contact optical measurement technique (Sutton *et al.* 2009, Lin and Labuz 2013). DIC has been used to monitor the displacement and strain of quasi-brittle materials by a number of researchers recently (Nguyen *et al.* 2011). Some researchers used DIC to investigate the damage evolution and fracture mechanism of rocks under various conditions (Zhou and Yang 2007, Gao *et al.* 2015)). The basic concept of DIC is particle tracking which is used to determine the displacement of particles in a digital image. By comparing two images acquired at different deformation stages or displacement fields, strains over the surface of a deforming material can be assessed (Song *et al.* 2013, La Rosa *et al.* 2017). The entire CCNBD testing process in this study was recorded using two calibrated cameras for DIC with a recording speed of 15 frames-per-second (fps). The DIC camera recording was synchronized with a MTS system to monitor the exact time and load corresponding to crack initiation and development (Fig. 2). The images obtained with the DIC cameras were used for both strain and crack propagation velocity measurements in each specimen.

2.5 Microstructure and clay composition analyses of calcite-cemented sandstone

FEI Quanta 600I environmental scanning electron microscope (ESEM) was employed to investigate the microstructural features of calcite cemented sandstone specimens. One representative specimen (divider, arrester and short transverse) from each of oven-dried and water-saturated conditions was selected for ESEM observation before and after CCNBD tests. Each specimen was coated with a thin gold film layer, and ESEM images were taken under a high vacuum chamber pressure of 0.9 Torr. ESEM images were taken directly on the surface of unloaded specimens and on the failure surface of loaded specimens.

X-ray diffraction (XRD) mineral analysis of the calcite-cemented sandstone was conducted to assess the mineral composition of the calcite-cemented sandstone including clay fraction. XRD analysis was performed with an automated power diffractometer equipped with a Cu radiation source (40kV, 40mA) and a solid state or scintillation detector. The quantitative determinations of whole-rock and phyllosilicate mineral amounts were carried out utilizing integrated peak areas (derived from peak-decomposition / profile-fitting methods) and empirical reference intensity ratio (RIR) factors determined specifically for the diffractometer used in data collection.

Table 1 Mechanical properties of calcite-cemented sandstone specimens. The values in parentheses are the standard error of the mean (SEM) ($3 \leq n \leq 6$)

Bedding orientation	Condition	Porosity (%)	Density (kN/m^3)	Avg. UCS (MPa)	Avg. BTS (MPa)	Avg. Young's modulus (GPa)
Parallel	Oven-dried	8.3 (± 0.05)	23.2 (± 0.05)	92.1 (± 2.7)	6.6 (± 0.1)	10.1 (± 0.17)
	Saturated		24.1 (± 0.05)	43.9 (± 1.8)	2.5 (± 0.3)	6.9 (± 0.22)
Perpendicular	Oven-dried	8.5 (± 0.06)	23.2 (± 0.04)	97.6 (± 0.7)	7.2 (± 0.5)	10.4 (± 0.03)
	Saturated		24.3 (± 0.03)	47.7 (± 0.1)	3.0 (± 0.1)	7.2 (± 0.12)

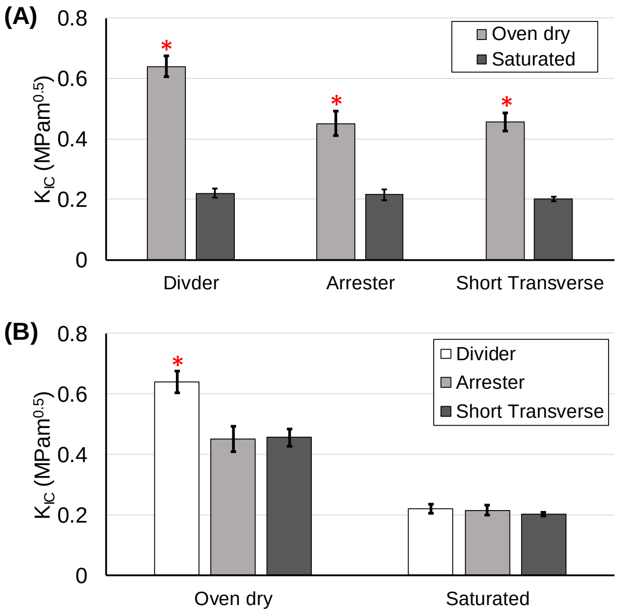

Fig. 3 Mode I fracture toughness (K_{IC}) of oven dried (control) and saturated CCNBD specimens along the three notch orientations. Comparisons of K_{IC} between (A) oven dry and saturated conditions and (B) notch orientations. * $P < 0.05$ (Student's one-tailed t-test). Error bars show SEM ($4 \leq n \leq 6$)

3. Results and discussion

3.1 Effects of water on strength and modulus

Mechanical properties of calcite-cemented sandstone specimens are shown in Table 1. The UCS and BTS of the calcite-cemented sandstone specimens in saturated condition decreased significantly when compared with oven-dried condition. When specimens were loaded parallel to the bedding plane, the UCS and BTS were reduced ~52% and ~62%, respectively. Meanwhile, the UCS and BTS were decreased ~51% and ~58%, respectively, when specimens were loaded perpendicular to the bedding plane. In addition, 32% reduction in Young's modulus (E_{t50}) was observed in saturated condition when compared with oven dry condition in both parallel and perpendicular loading conditions. The results support the conclusion that water saturation greatly decreases mechanical strengths of the tested calcite-cemented sandstone specimens regardless of bedding plane anisotropy, showing that the tested calcite-cemented sandstone is very sensitive to water.

The strength reduction in sandstones due to the presence of moisture have been extensively researched (Mann and Fatt 1960, Kim and de Oliveira 2015, Kim *et al.* 2018). According to previous reports, the reduction in UCS ranged from ~10 to ~90%, Young's modulus ranged from ~10 to ~70%, and BTS ranged from ~11% to ~65% due to the presence of water. Several explanations were put forward to describe the effects of water on mechanical strength reduction in sandstones. Inherent microstructural features, such as the geometry of grain boundaries, pore spaces, and grain-matrix relation (i.e., presence or absence of clayey matrix) were found to have considerable impacts on moisture-related strength reduction in sandstones. The presence of water in sandstones can induce stress corrosion which converts strong silica-oxygen bonds to much weaker hydrogen bonds: (–Si–O–Si–) + (H–O–H) = (–Si–OH·OH–Si) (Zhou *et al.* 2018), indicating that water is one of key factors in reducing the mechanical strength of sandstones.

Additionally, compressive strength, tensile strength and Young's modulus did not significantly differ between parallel and perpendicular bedding orientations in both saturated and oven-dried specimens based on p-values since p-values were higher than 0.05 (data not shown). This indicates that the strength anisotropy of the tested calcite-cemented sandstone along bedding directions is insignificant.

3.2 Effects of water on mode I fracture toughness (K_{IC})

Fracture toughness (K_{IC}) obtained from oven-dried and saturated calcite-cemented sandstone specimens along the three notch orientations (divider, arrester and short transverse) are shown in Fig.1. In divider specimens, K_{IC} was significantly lower (~66%) in saturation condition than oven dry condition (Fig. 3). In arrester and short transverse specimens, K_{IC} was ~52% and ~ 56% lower in saturated specimens than oven-dried specimens, respectively. The results clearly reveal that water can drastically decrease fracture toughness of the calcite-cemented sandstone regardless of bedding plane directions. This observation can be explained that water saturation of the calcite-cemented sandstone can create more microcracks and void spaces, resulting in the strength disparity between cement and rock forming mineral grains (Lin *et al.* 2005). This supports the evidence that water can reduce the crack propagation resistance of the sandstone leading to lower K_{IC}.

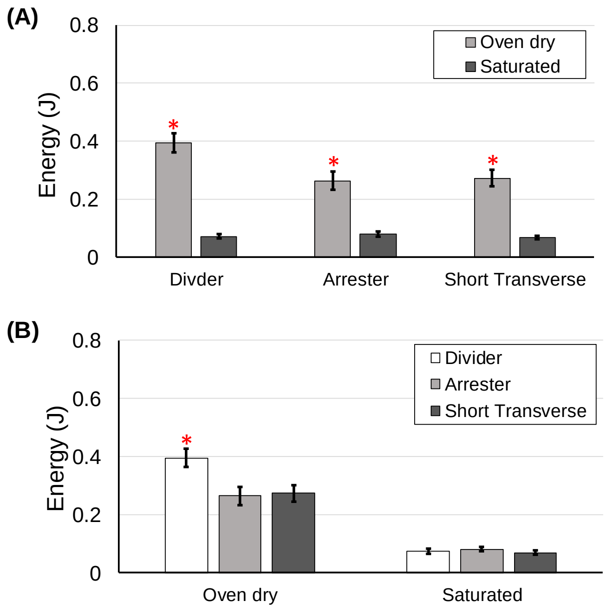

Fig. 4 Consumed energy for oven dry and saturated specimens along the three notch orientations. Comparisons of consumed energy between (A) oven dry and saturated conditions and (B) bedding plane orientations. * P < 0.05 (Student's one-tailed t-test). Error bar is SEM (4 ≤ n ≤ 6)

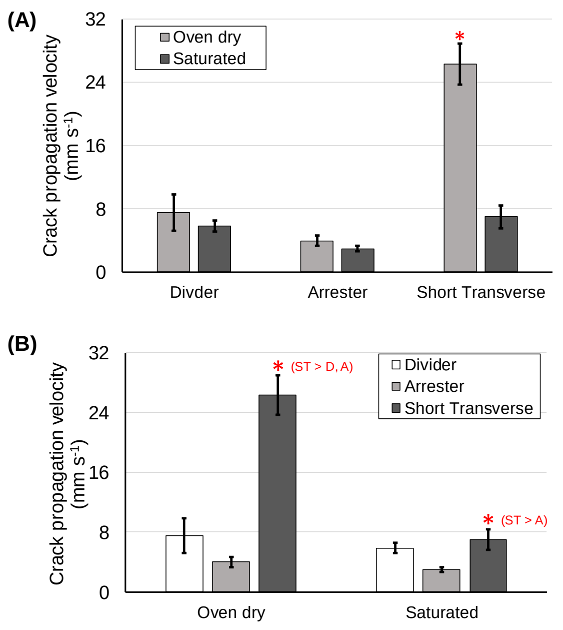

Fig. 6 Crack propagation velocities for oven dried and saturated specimens along the three notch orientations. Comparisons of crack propagation velocity between (A) oven dry and saturated conditions and (B) bedding plane orientations. * P < 0.05 (Student's one-tailed t-test). Error bar is SEM (*n* = 10).

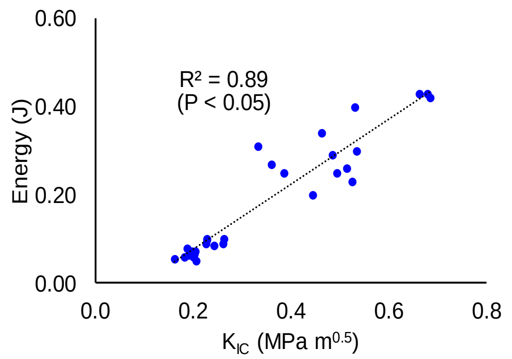

Fig. 5 Correlation analysis between the consumed energy and mode I fracture toughness (K_{IC}) of oven-dried and saturated samples. Each data point represents the average value of the consumed energy and K_{IC} of divider, arrester or short transverse samples

The energy consumed during the failure process was examined for each specimen by calculating the area under the force-displacement curve measured during CCNBD tests. The K_{IC} for divider specimens in oven dry condition revealed statistically higher than arrester and short transverse specimens (Fig. 3). Whereas, in saturated condition, K_{IC} did not statistically differ with respect to bedding plane orientations (divider, arrester and short transverse). The results suggest that water saturation can significantly decrease the anisotropic bedding effect on fracture toughness. To date we do not fully understand why the effect of bedding plane orientations on fracture toughness is markedly greater in dry condition than saturated condition although it is likely that the bedding effect on fracture toughness is weaker as fracture toughness is lower. Accordingly, we expect that other conditions such as heat, cycling loadings (fatigue), and repeated freeze and thaw which reduce fracture toughness can also weaken the effect of bedding plane orientations on fracture toughness. In future it is necessary to examine how the bedding effect on fracture mechanics is correlated with the changes of rock mechanical strengths. In addition, we do not fully understand what grains and grain boundaries are more sensitive to water, leading to the reduction of geomechanical strengths. Thus, it is also necessary to study what grains and grain boundaries play critical roles in the reduction of water-mediated geomechanical strengths.

Additionally, it is noticeable that the effect of bedding orientations on mechanical strengths was not obvious in dry condition (Table 1); however, the effect on fracture toughness was statistically significant in dry specimens. The results clearly support the evidence that fracture toughness is more sensitive to bedding plane orientations when comparing to mechanical strengths, especially in dry condition. Conversely, rock fracturing processes can be substantially affected by bedding plane orientations; thus, it is critical to understand rock fracturing behaviors depending on bedding anisotropy.

The consumed energy used in the failure process of saturated divider, arrester and short transverse specimens was estimated by calculating the area under the load-displacement curve obtained during CCNBD tests. The energy consumed during the failure process in saturated divider, arrester and short transverse specimens was 81%, 69% and 75% lower than that of oven-dried specimens. This supports the conclusion that water saturation reduces the crack propagation resistance of the rock, so less energy is required in saturated specimens for crack growth than in

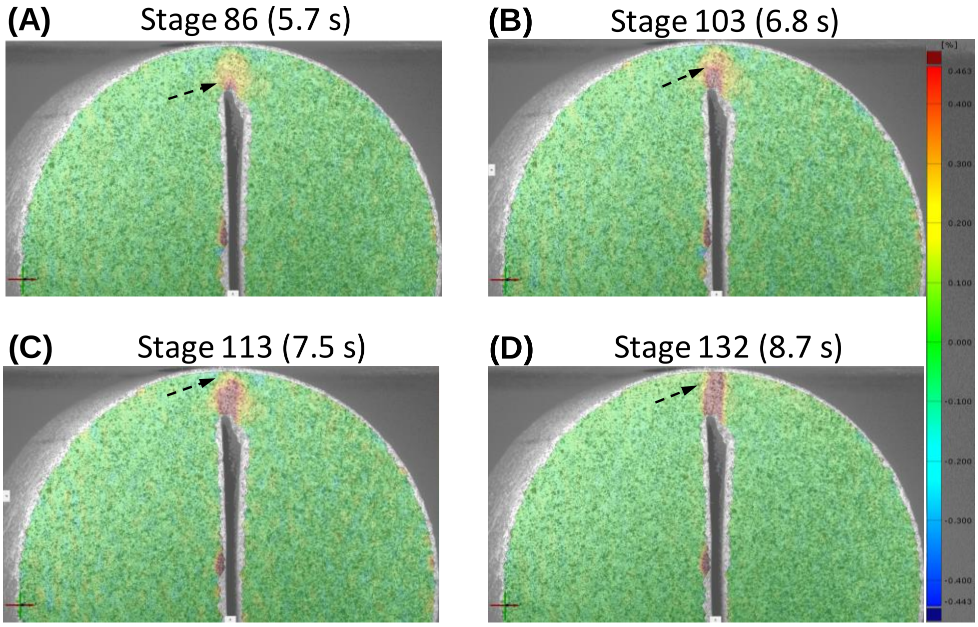

Fig. 7 Crack propagation observed using DIC images in an exemplary saturated specimen (A)-(D). The time shown here is from the start of loading. Arrow shows the crack front at different stages

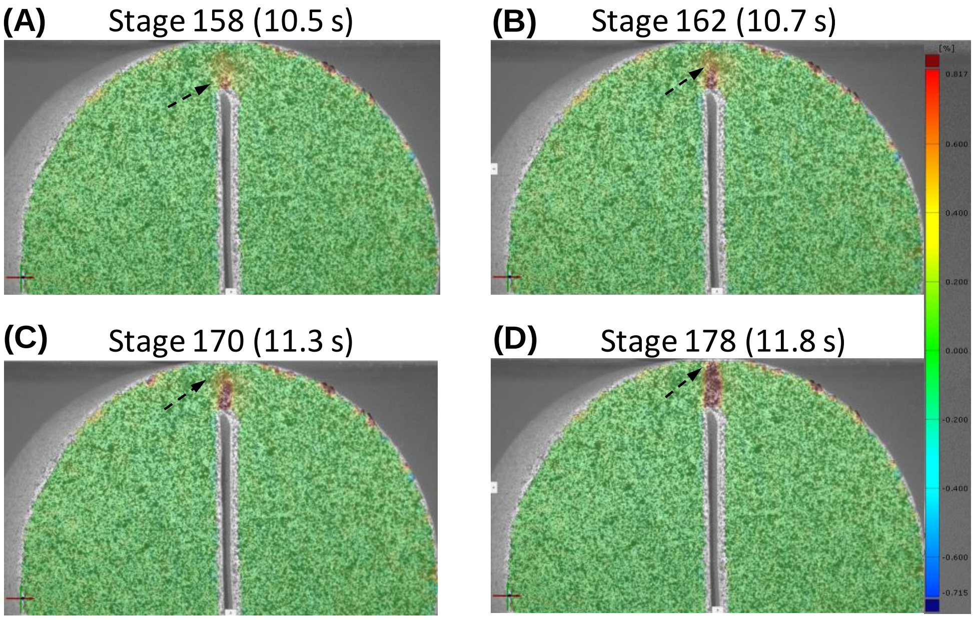

Fig. 8 Crack propagation observed using DIC images in an exemplary oven-dried specimen (A)-(D). The time shown here is from the start of loading. Arrow shows the crack front at different stages

oven-dried specimens. Also, consistent with K_{IC}, consumed energy in water-saturated specimens did not significantly differ with respect to the three notch orientations (Fig. 4).

As the consumed energy and K_{IC} in dried and saturated specimens show quite similar patterns with the changes of the three bedding orientations, we analyzed the correlation between the consumed energy and K_{IC}. Noticeably, the consumed energy during rock failure process is highly correlated with mode I fracture toughness (Fig. 5), suggesting that more energy is required for breaking a rock with higher fracture toughness. For application aspects, this result provides insightful information to estimate the appropriate energy for rock aggregate or fragment production.

3.3 Effects of water on crack propagation velocity

Crack propagation velocity was measured using DIC images recorded during CCNBD tests. Initially, a strain contour plot was generated by comparing the DIC images acquired at different deformation steps. Crack tips can be identified as regions of maximum strain values in strain contour plots, and crack propagation velocity can be calculated by comparing the length of crack tips at different time frames. The crack propagation velocity in saturated specimens was found to be lower than oven-dried specimens. Significant reduction in crack propagation velocity was observed in short transverse specimens due to saturation. The average crack propagation velocity in saturated short transverse specimens was 73% lower than oven-dried short transverse specimens, whereas in divider and arrester specimens the reduction in crack propagation velocity was not statistically significant; although the average crack propagation velocity in saturated divider and arrester specimens were 22% and 25% lower than oven-dried divider and arrester specimens, respectively (Fig. 6). Intriguingly, the crack propagation velocity in saturated specimens varied with the three notch orientations. In saturated specimens, the crack velocity was faster in short transverse specimens and slower in arrester, and intermediate crack velocity was observed in divider even though the consumed energy and K_{IC} were similar regardless of the bedding plane orientations (Fig. 4(B)) and 6(B)). The results suggest that crack propagation velocity is mainly determined by bedding plane orientation rather than K_{IC} or consumed energy in the saturated sandstone.

Consistent with the saturated specimens, the order of the crack propagation velocity in the oven-dried specimens was short transverse, divider, and arrester. Currently, we do not completely understand why the crack propagation velocity is faster in short transverse and slower in arrester; however, it appears that bedding plane orientation is a critical factor in determining crack propagation velocity as the notch orientation of arrester specimens is perpendicular to the bedding orientation—slower crack velocity—while parallel in short transverse specimens—faster crack velocity. In other words, crack velocity is faster when the bedding plane orientation is the same direction as the crack propagation while the crack velocity is slower when the bedding orientation is perpendicular to the crack growth direction.

From strain contour images, it was observed that crack initiation in saturated specimen started at stage 86 (t = 5.7 s), and this crack was fully developed at stage 132 (t = 8.7 s) (Fig. 7). In oven-dried specimen crack initiation started at stage 158 (t = 10.5 s), and the crack was fully developed at stage 178 (t = 11.8 s) (Fig. 8). To sum up, the crack in the saturated specimen initiated at initial stages of loading but took more time for its full development (~3 s) while the crack in the oven-dried specimen initiated at a much later stage of loading and fully developed much quicker (~1.3 s). Our findings support the conclusion that when the calcite-cemented sandstone is saturated, crack initiation occurs at lower stress, but crack development is slower, when compared with dried specimens. Our data are very interesting and important in two aspects: (1) if cracks are once initiated in dry condition, rock mass failure can be quicker than in saturation condition, and (2) the rock mass failure can occur at lower stress condition when saturated.

Here one may raise a question about how crack development is faster in dry condition than in saturated condition. This can be explained with that the crack development occurs at lower stress in saturation condition than dry condition, so that crack propagation velocity is slower in saturated specimens than dry samples as shown in Fig. 6. Also, one may wonder whether the loss of geomechanical strengths could be recovered when the saturated rock specimen was oven-dried again. We have not tested whether the effect of water saturation on the geomechanical strengths could be a reversible process. The reduction of the geomechanical strengths by water saturation is mediated by multiple factors such as water pore pressure, clay expansion, and calcite dissolution. Water pore pressure and clay expansion could be reversible, but calcite dissolution could be an irreversible process. Thus, we predict that the water saturation effect could be somewhat recovered, but not completely recovered after oven-drying the saturated rock sample.

3.4 Effect of water saturation on rock microstructure

ESEM images were used for the assessment of microstructural damages produced by oven dry and water saturation before and after CCNBD tests. Qualitative assessment of microstructural damages based on ESEM images was performed for each group of specimens. ESEM images of water-saturated specimens before CCNBD tests showed significant differences in terms of microscale damages when compared with oven-dried specimens. Several voids were visible along the grain boundaries and on the exposed mineral surfaces in water-saturated calcite-cemented sandstone specimens due to the dissolution and/or leaching of minerals (Fig. 9).

From the XRD data of the calcite-cemented sandstone, quartz was found to be the major rock forming mineral followed by plagioclase, calcite, dolomite, K-feldspar and clay minerals (Fig. 10). Previous researches reported dissolution and/or leaching of K-feldspar and chlorite minerals from the rock in presence of water/moisture. Circular holes are produced on the exposed feldspar mineral surface which enlarge to form ring-shaped structures and later develop into large holes (Eggleton and Buseck 1980). Microcracks was also observed due to the expansion of clay minerals in presence of water (Fig. 9(c)). The clay mineral content present in the calcite-cemented sandstone was 18.2% (Fig. 11). Based on the volume fraction of clay minerals (V_{clay}), the calcite-cemented sandstone can be grouped into a transitional-support rock (15% < V_{clay} < 35%) (Dott Jr 1964, Picard 1971). In transitional-support rocks, loads are more equally distributed among clay minerals and detrital grains, when compared with grain-support rocks containing clay minerals less than 15% (V_{clay} < 15%) (Plumb 1994, Kim *et al.* 2017). Thus, relatively high clay content of the calcite-cemented sandstone can enhance the effect of water on fracturing behaviors as well as the reduction of mechanical strengths.

The clay of the calcite-cemented sandstone consists mainly of kaolinite and corrensite minerals along with mixed layer of illite-smectite and illite-mica. According to a previous research, a volume expansion of 14% was reported in corrensite mineral in the presence of water (Lippmann 1976). Mooney and his co-researchers reported that smectites were able to expand up to half of their mass in presence of water (Mooney *et al.* 1952). When hydrated, the inner OH groups of kaolinite can be disturbed, forcing water molecules to enter into kaolinite structure (Costanzo *et al.* 1984). In addition, water can penetrate the ditrigonal cavities of kaolinite and perturb inner OH groups creating

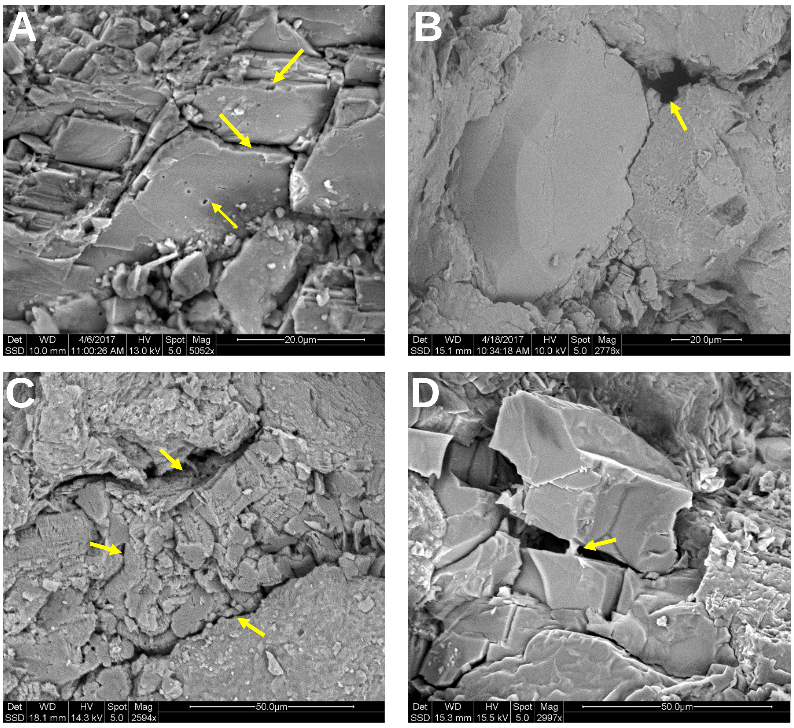

Fig. 9 ESEM images showing microscale damages in calcite-cemented sandstones due to water saturation. (A) Dissolution of K-feldspar mineral along the grain boundaries and on the exposed surface (B) void space created due to complete dissolution of mineral grain. Note the microcrack developed along the grain boundary connecting the void space (C) microcrack created due to expansion of clay minerals and (D) partial dissolution of a mineral grain

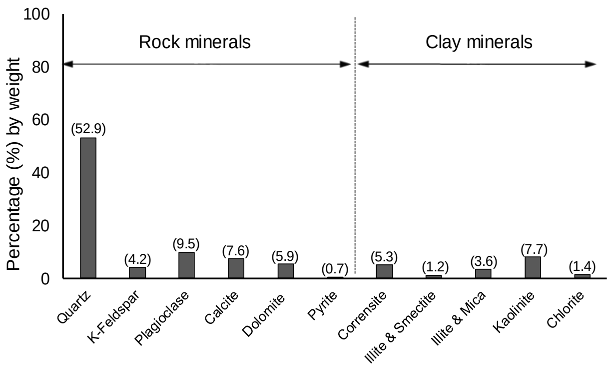

Fig. 10 XRD analysis result of calcite cemented sandstone. Each number in parenthesis indicates a percentage (%, w/w) value of rock or clay mineral

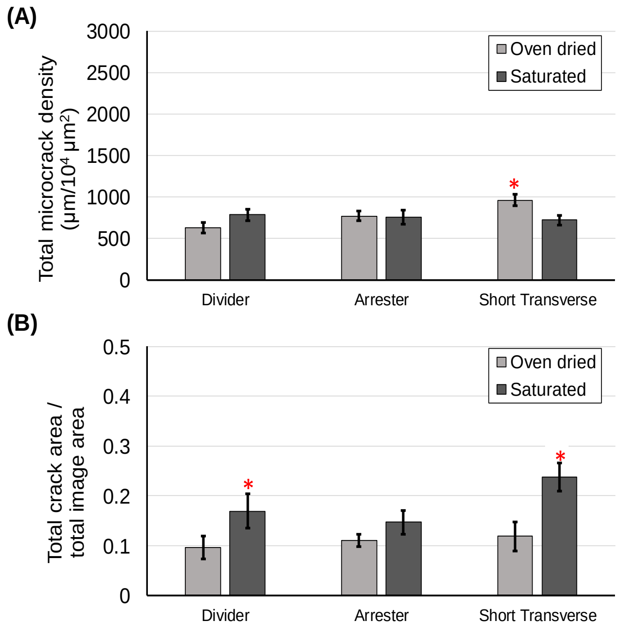

Fig. 11 Microcrack density for oven-dried and water-saturated specimens. (A) Total microcrack density (total length per area) and (B) the ratio of total crack area to total picture area of oven-dried (control) and saturated CCNBD samples along three bedding orientations. * $P < 0.05$ (Student's one-tailed *t*-test). Error bars indicate SEM ($n = 10$)

microfractures (Xu *et al.* 2000).

Both qualitative and quantitative microstructural damages—based on ESEM images—were analyzed for specimens after CCNBD tests. Quantitative assessment of microstructural damages was performed by calculating the total microcrack density and microcrack area produced in the specimens after the CCNBD tests, which was conducted using MATLAB codes written for ESEM image processing. The microcrack length was calculated as the ratio of total crack length to total picture area (Fig. 11(A)). The microcrack area produced in the specimens was expressed as the ratio of total microcrack area to total picture area (Fig. 11(B)).

For microcrack length, the significant difference between oven-dried and saturated samples were not observed in divider and arrester. Surprisingly, in short transverse orientation, more microscale crack as length

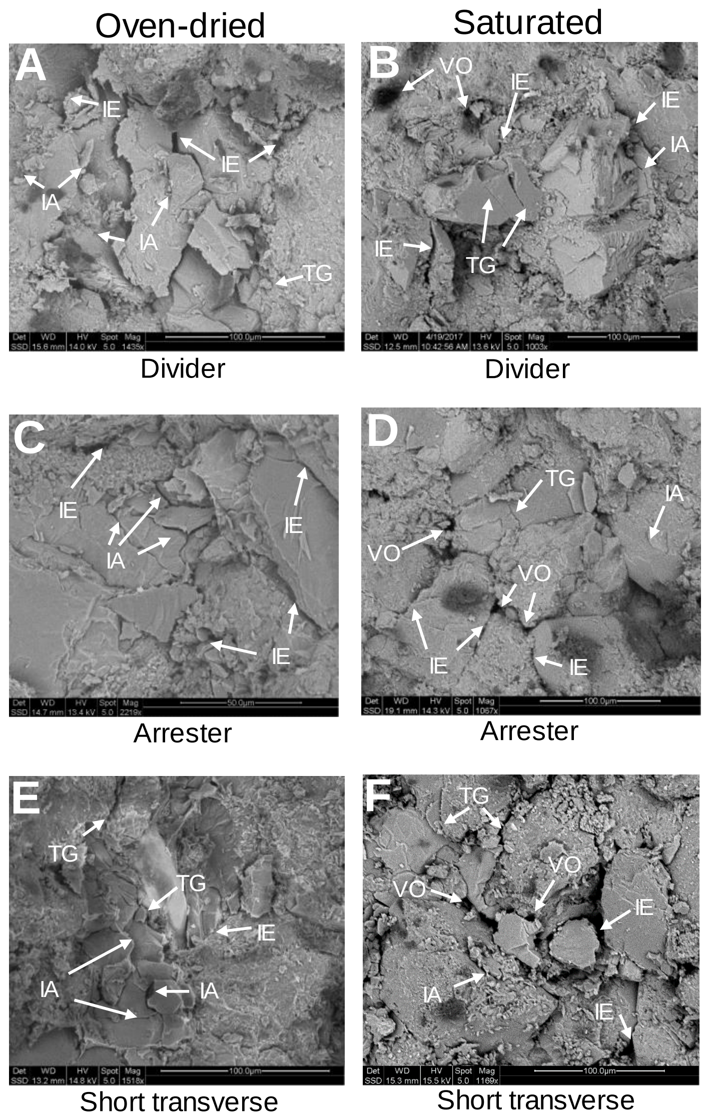

Fig. 12 Microscale crack images of calcite cemented sandstone after CCNBD test taken with ESEM in three bedding directions. (A), (C), and (E) images were taken from oven-dried specimens, and (B), (D), and (F) images were taken from water-saturated specimens (IE: intergranular crack, IA: intragranular crack, TG: transgranular, VO: void)

(~25%) was observed in oven-dried specimens than saturated specimens, which was totally unexpected (Fig. 11(a)). We expected water will increase microcrack length because water molecules can expand clays, increase pore pressure, and dissolve calcite of the rock. To understand how water saturation can decrease microcrack length, we investigated microcrack area. Interestingly, the microcrack area in water-saturated specimens for divider, arrester and short transverse was found to be ~77%, ~34%, and ~100% larger than oven-dried specimens, respectively (Fig. 11). To sum up, water saturation can reduce the microcrack length but increase the microcrack area after CCNBD tests, when compared with oven dry condition. The results suggest that water saturation enhances the coalescence of microscale cracks or grain separation creating wide microcracks. ESEM observation supports this interpretation. For saturated specimens, ESEM images showed that microcrack concentration was lower in mineral grains when compared to matrix. The mineral grains were intact and suffered less damage (Fig. 12(B), 12(D) and 12(F)). The microcracks along grain boundaries in water-saturated specimens were fully developed with considerable separation. The above observations prove that water saturation in the calcite-cemented sandstone increased the strength difference between matrix and mineral grains resulting in the moving of grains along failure planes when loaded as opposed to fracturing through mineral grains (Hawkins and McConnell 1992). In addition, the coalescence of microcracks and linkage of adjacent void spaces were observed in water-saturated specimens (Fig. 12(D) and 12(F)). Whereas, it seemed that more mineral grains were fractured in oven-dried specimens when compared with saturated specimens (Fig. 12(A), 12(C) and 12(E)). The separation of grain boundaries was not widespread as in saturated specimens. However, in oven- dried specimens, microcrack coalescence was visible, but no void spaces were observed. Our findings provide insights into how water affects the stability of geostructures, especially in calcite-rich geostructures since calcite is extremely sensitive to water.

4. Conclusions

In this study, the effects of water on fracturing behaviors were examined in the calcite-cemented sandstone. Water saturation of the calcite-cemented sandstone was found to have a significant effect on geo-mechanical properties, mode I fracture toughness (K_{IC}), consumed energy, and crack propagation velocity. The UCS, BTS and Young's modulus (E_{t50}) of the calcite-cemented sandstone specimens in saturation condition decreased significantly when compared with oven dry condition. Mode I fracture toughness (K_{IC}) and consumed energy were substantially reduced when specimens were saturated. For divider, arrester and short transverse specimens, K_{IC} in saturation condition was 66%, 52% and 56% lower than oven dry condition, respectively. The average consumed energy in water-saturated divider, arrester and short transverse specimens were 81%, 69% and 75% lower than the respective oven-dried specimens. The consumed energy during rock failure is highly correlated with the fracture toughness (R^2 = 0.89). The crack propagation velocity in saturated specimens was found to be lower than oven-dried specimens. Overall the crack propagation velocity was faster in short transverse and slower in arrester, and intermediate in divider specimens although the consumed energy and K_{IC} were similar regardless of the bedding plane orientations supporting the conclusion that crack propagation velocity is mainly determined by bedding plane orientation in the saturated calcite-cemented sandstone. This suggests that bedding plane orientation should be seriously considered when examining fracturing behaviors and assessing the stability of geostructures.

In addition, based on strain contour data, when the calcite-cemented sandstone is saturated, crack initiation occurs at lower stress, and crack development is slower when compared with dried specimens. This can be explained with that crack development occurs at lower stress in saturation condition than dry condition, so that crack propagation velocity is slower in saturated specimens than dry samples. Thus, it is concluded that if cracks are once initiated in dry condition, rock mass failure can be quicker than in saturation condition, and the rock mass failure can occur lower stress condition when saturated.

When loaded, more excessive microcrack coalescence and linkage of adjacent void spaces were observed in water-saturated specimens when compared with oven-dried specimens. Increased the strength disparity between cement and rock forming mineral grains seemed to reduce the crack propagation resistance of the sandstone leading to lower consumed energy and K_{IC}. Our findings in this study provide insights into understanding the effects of water on rock fracturing processes along the orientation of rock bedding plane.

Acknowledgements

The authors thank our lab coordinators and student helpers at Colorado School of Mines (CSM) for their technical assistance. We also appreciate the support of Center for Underground Construction and Tunneling (UCT) and UCT Engineering Program which provided excellent opportunities to Varun Maruvanchery, and a CSM seed grant to Dr. Eunhye Kim (Department of Mining Engineering).

References

Anderson, T.L. (2017), *Fracture Mechanics: Fundamentals and Applications*, CRC press.

ASTM D3967-16 (2016), *Standard Test Method for Splitting Tensile Strength of Intact Rock Core Specimens*, West Conshohocken, Pennsylvania, U.S.A.

ASTM D4543-08 (2008), *Standard Practices for Preparing Rock Core as Cylindrical Test Specimens and Verifying Conformance to Dimensional and Shape Tolerances*, West Conshohocken, Pennsylvania, U.S.A.

Behrens, H. and Müller, G. (1995), "An infrared spectroscopic study of hydrogen feldspar (HAlSi3O8)", *Mineralog. Mag.*, **59**(1), 15-24.

Chang, S.H., Lee, C.I. and Jeon, S. (2002), "Measurement of rock fracture toughness under modes I and II and mixed-mode conditions by using disc-type specimens", *Eng. Geol.*, **66**(1-2), 79-97.

Costanzo, P., Giese, R. and Lipsicas, M. (1984), "Static and dynamic structure of water in hydrated kaolinites; I, The static structure", *Clay. Clay Miner.*, **32**(5), 419-128.

Detournay, E. (2016), "Mechanics of hydraulic fractures", *Ann. Rev. Fluid Mech.*, **48**(1), 311-339.

Dott Jr, R.H. (1964), "Wacke, Graywacke and matrix—what approach to immature sandstone classification?", *J. Sediment. Res.*, **34**(3), 625-632.

Dyke, C.G. and Dobereiner, L. (1991), "Evaluating the strength and deformability of sandstones", *Quart. J. Eng. Geol. Hydrogeol.*, **24**, 123-134.

Eggleton, R. and Buseck, P. (1980), "High resolution electron microscopy of feldspar weathering", *Clay. Clay Miner.*, **28**(3), 173-178.

Erguler, Z. and Ulusay, R. (2009), "Water-induced variations in mechanical properties of clay-bearing rocks", *Int. J. Rock Mech. Min. Sci.*, **46**(2), 355-370.

Feng, X.T., Ding, W.X. and Zhang, D.X. (2009), "Multi-crack interaction in limestone subject to stress and flow of chemical solutions", *Int. J. Rock Mech. Min. Sci.*, **46**(1), 159-171.

Feng, X.T., Li, S.J. and Chen, S.L. (2004), "Effect of water chemical corrosion on strength and cracking characteristics of rocks-a review", *Key Eng. Mater.*, **261-263**, 1355-1360.

Fowell, R.J. (1995), "Suggested method for determining mode I fracture toughness using Cracked Chevron Notched Brazilian Disc (CCNBD) specimens", *Int. J. Rock Mech. Min. Sci. Geomech. Abstr.*, **32**(1), 57-64.

Fowell, R.J. and Xu, C. (1994), "The use of the cracked Brazilian disc geometry for rock fracture investigations", *Int. J. Rock Mech. Min. Sci. Geomech. Abstr.*, **31**(6), 571-579.

Fyfe, W.S., Price, N.J. and Thompson, A.B. (1978), *Fluids in the Earth's crust. Developments in Geochemistry 1*, Elsevier, 3-4.

Gao, G., Huang, S., Xia, K. and Li, Z. (2015), "Application of digital image correlation (DIC) in dynamic notched semi-circular bend (NSCB) tests", *Exp. Mech.*, **55**(1), 95-104.

Gonzáles, G.L., González, J.A., Castro, J.T. and Freire, J.L. (2017), "A J-integral approach using digital image correlation for evaluating stress intensity factors in fatigue cracks with closure effects", *Theor. Appl. Fract. Mech.*, **90**, 14-21.

Gupta, M., Alderliesten, R.C. and Benedictus, R. (2015), "A review of T-stress and its effects in fracture mechanics", *Eng. Fract. Mech.*, **134**, 218-241.

Hadizadeh, J. and Law, R.D. (1991), "Water-weakening of sandstone and quartzite deformed at various stress and strain rates", *Int. J. Rock Mech. Min. Sci. Geomech. Abstr.*, **28**(5), 431-439.

Hawkins, A.B. and Mcconnell, B.J. (1992), "Sensitivity of sandstone strength and deformability to changes in moisture content", *Quart. J. Eng. Geol.*, **25**(2), 115-130.

Karakul, H. and Ulusay, R. (2013), "Empirical correlations for predicting strength properties of rocks from p-wave velocity under different degrees of saturation", *Rock Mech. Rock Eng.*, **46**(5), 981-999.

Kim, E. and Changani, H. (2016), "Effect of water saturation and loading rate on the mechanical properties of Red and Buff Sandstones", *Int. J. Rock Mech. Min. Sci.*, **88**, 23-28.

Kim, E. and De Oliveira, D.B.M. (2015), "The effects of water saturation on dynamic mechanical properties in red and buff sandstones having different porosities studied with Split Hopkinson Pressure Bar (SHPB)", *Appl. Mech. Mater.*, **752**, 784-789.

Kim, E., Garcia, A. and Changani, H. (2018), "Fragmentation and energy absorption characteristics of Red, Berea and Buff sandstones based on different loading rates and water contents", *Geomech. Eng.*, **4**(2), 151-159.

Kim, E., Stine, M.A., De Oliveira, D.B.M. and Changani, H. (2017), "Correlations between the physical and mechanical properties of sandstones with changes of water content and loading rates", *Int. J. Rock Mech. Min. Sci.*, **100**, 255-262.

Knauss, W.G. (2015), "A review of fracture in viscoelastic materials", *Int. J. Fract.*, **196**(1-2), 99-146.

La Rosa, G., Clienti, C., Marino Cugno Garrano, A. and Lo Savio, F. (2017), "A novel procedure for tracking the measuring point in thermoelastic curves using D.I.C.", *Eng. Fract. Mech.*, **183**, 53-65.

Labuz, J.F., Shah, S.P. and Dowding, C.H. (1985), "Experimental analysis of crack propagation in granite", *Int. J. Rock Mech. Min. Sci. Geomech. Abstr.*, **22**(2), 85-98.

Le, J.L., Manning, J. and Labuz, J.F. (2014), "Scaling of fatigue crack growth in rock", *Int. J. Rock Mech. Min. Sci.*, **72**, 71-79.

Lim, I.L., Johnston, I.W., Choi, S.K. and Boland, J.N. (1994), "Fracture testing of a soft rock with semi-circular specimens under three-point bending. Part 1—mode I", *Int. J. Rock Mech. Min. Sci. Geomech. Abstr.*, **31**(3), 185-197.

Lin, M.L., Jeng, F.S., Tsai, L.S. and Huang, T.H. (2005), "Wetting weakening of tertiary sandstones—microscopic mechanism", *Environ. Geol.*, **48**(2), 265-275.

Lin, Q. and Labuz, J.F. (2013), "Fracture of sandstone characterized by digital image correlation", *Int. J. Rock Mech. Min. Sci.*, **60**, 235-245.

Lippmann, F. (1976), "Corrensite, a swelling clay mineral, and its influence on floor heave in tunnels in the Keuper formation", *Bull. Int. Assoc. Eng. Geol.*, **14**(1), 65-68.

Liu, M. and Chen, C. (2015), "A micromechanical analysis of the fracture properties of saturated porous media", *Int. J. Solids Struct.*, **63**, 32-38.

Mann, R. and Fatt, I. (1960), "Effect of pore fluids on the elastic properties of sandstone", *Geophysics*, **25**(2), 433-444.

Mooney, R., Keenan, A. and Wood, L. (1952), "Adsorption of water vapor by montmorillonite. II. Effect of exchangeable ions and lattice swelling as measured by X-ray diffraction", *J. Am. Chem. Soc.*, **74**(6), 1371-1374.

Nara, Y., Meredith, P.G., Yoneda, T. and Kaneko, K. (2011), "Influence of macro-fractures and micro-fractures on permeability and elastic wave velocities in basalt at elevated pressure", *Tectonophysics*, **503**(1-2), 52-59.

Nasseri, M.H.B. and Mohanty, B. (2008), "Fracture toughness anisotropy in granitic rocks", *Int. J. Rock Mech. Min. Sci.*, **45**(2), 167-193.

Nguyen, T.L., Hall, S.A., Vacher, P. and Viggiani, G. (2011), "Fracture mechanisms in soft rock: Identification and quantification of evolving displacement discontinuities by extended digital image correlation", *Tectonophysics*, **503**(1-2), 117-128.

Picard, M.D. (1971), "Classification of fine-grained sedimentary rocks", *J. Sediment. Res.*, **41**(1), 179-195.

Plumb, R.A. (1994), *Influence of Composition and Texture on the Failure Properties of Clastic Rocks*, in *Rock Mechanics in Petroleum Engineering*, Society of Petroleum Engineers, Delft, The Netherlands.

Schmidt, R.A. (1976), "Fracture-toughness testing of limestone", *Exp. Mech.*, **16**(5), 161-167.

Schumacher, F.P. and Kim, E. (2013), "Modeling the pipe umbrella roof support system in a Western US underground coal mine", *Int. J. Rock Mech. Min. Sci.*, **60**, 114-124.

Shakoor, A. and Barefield, E.H. (2009), "Relationship between unconfined compressive strength and degree of saturation for selected sandstones", *Environ. Eng. Geosci.*, **15**(1), 29-40.

Song, H., Zhang, H., Kang, Y., Huang, G., Fu, D. and Qu, C. (2013), "Damage evolution study of sandstone by cyclic uniaxial test and digital image correlation", *Tectonophysics*, **608**, 1343-1348.

Sutton, M.A., Orteu, J.J. and Schreier, H.W. (2009), *Image Correlation for Shape, Motion and Deformation Measurements: Basic Concepts, Theory and Applications*, Springer.

Thompson, T.A., Sowder, K.H. and Johnson, M. (2013), *Generalized Stratigraphic Column of Indiana Bedrock: Indiana Geological Survey Poster*, Indiana Geological Survey: Bloomington, Indiana, U.S.A.

Tracy, J., Waas, A. and Daly, S. (2015), "Experimental assessment of toughness in ceramic matrix composites using the J-integral with digital image correlation part II: Application to ceramic matrix composites", *J. Mater. Sci.*, **50**(13), 4659-4671.

Vásárhelyi, B. and Ván, P. (2006), "Influence of water content on the strength of rock", *Eng. Geol.*, **84**(1-2), 70-74.

Verstrynge, E., Adriaens, R., Elsen, J. and Van Balen, K. (2014), "Multi-scale analysis on the influence of moisture on the mechanical behavior of ferruginous sandstone", *Construct. Build. Mater.*, **54**(Supplement C), 78-90.

Weaver, C.E. (1989), *Clays, Muds, and Shales: Development in Sedimentology*, 44, Elsevier.

Xu, W., Johnston, C.T., Parker, P. and Agnew, S.F. (2000), "Infrared study of water sorption on Na-, Li-, Ca-, and Mg-exchanged (SWy-1 and SAz-1) montmorillonite", *Clay. Clay Miner.*, **48**(1), 120-131.

Yoneyama, S., Arikawa, S., Kusayanagi, S. and Hazumi, K. (2014), "Evaluating J-integral from displacement fields measured by digital image correlation", *Strain*, **50**(2), 147-160.

Zhang, Z.X. (2016), *Environmental Effects on Rock Fracture*, in *Rock Fracture and Blasting*, Butterworth-Heinemann, 135-153.

Zhou, X.P. and Yang, H.Q. (2007), "Micromechanical modeling of dynamic compressive responses of mesoscopic heterogenous brittle rock", *Theor. Appl. Fract. Mech.*, **48**(1), 1-20.

Zhou, Z., Cai, X., Ma, D., Cao, W., Chen, L. and Zhou, J. (2018), "Effects of water content on fracture and mechanical behavior of sandstone with a low clay mineral content", *Eng. Fract. Mech.*, **193**, 47-65.

CC